Sensors and Materials, Vol. 29, No. 5 (2017) 567–573
MYU Tokyo

S & M 1350

Development of a Bead-Based Multiplexed Immunoassay Using Image Cytometric Analysis

Yoshiaki Ukita,[1*] Chiwa Kataoka,[2,3] Kazuyuki Sawadaishi,[3]
Akinobu Yamaguchi,[2] and Yuichi Utsumi[2]

[1]Faculty of Engineering, Graduate Faculty of Interdisciplinary Research, Graduate School of University of Yamanashi, 4-3-11 Takeda, Kofu, Yamanashi 400-8511, Japan
[2]Laboratory of Advances Science and Technology for Industry (LASTI), University of Hyogo, 3-1-2 Koto, Kamigori, Ako-gun, Hyogo 678-1205, Japan
[3]Carbuncle BioScienTec LLC., 40-26 Tanida, Okukaiinji, Nagaokakyo, Kyoto 617-0853, Japan

(Received December 13, 2016; accepted March 9, 2017)

Keywords: multiplexed immunoassay image cytometry, bead-based assay

In this paper, we present the demonstration of a size-encoded bead-based multiplexed immunoassay with image cytometric decoding and readout. Antibodies were immobilized on polystyrene microspheres by physical adsorption and employed for the demonstration of this duplexed immunoassay. First, we carried out a duplexed immunoassay with a mouse and rat IgG detection system and discussed the problem of cross-reactivity inherent to these immunoreaction systems. We then carried out a duplexed immunoassay with a mouse IgG and human albumin detection system, which was less cross-reactive. We subsequently demonstrated the application of size-encoded image cytometric decoding and the detection of mouse IgG and human albumin using this duplexed immunoassay system.

1. Background

Immunoassays are one type of analytical method, which are widely applied for the detection and quantitation of proteins, owing to their simplicity and high sensitivity.[1–4] Recent progress in proteomics has revealed correlations among disease, bioactivity, and molecular information, and this has strongly motivated the clinical application of multiplexed protein assay methods.[5–7] Protein microarrays, which are based on specific antibodies, are the ideal tool for multiplexed immunoassays.[8,9] A spot of antibody is printed locally using microprinting technology for the application of conventional, but multiplexed, immunoreactions. Therefore, antibody printing is becoming the main technical difficulty in carrying out these assays. Moreover, the reaction kinetics are relatively slow owing to the lengthy diffusion of molecules, because the reaction is carried out on a planar surface.[10,11]

As an alternative technique, bead-based multiplexed immunoassays have been intensively researched to overcome the drawbacks of microarray technology.[12–15] In the case of bead-based immunoassays, multiplexing is achieved by preparing multiple antibody-immobilized beads corresponding to each analyte, and thus multiplexed immunoreactions can be implemented

*Corresponding author: e-mail: yukita@yamanashi.ac.jp
http://dx.doi.org/10.18494/SAM.2017.1559

ISSN 0914-4935

in a single reaction chamber. This makes it possible to carry out these reactions in low sample volumes by suspending the microbeads in a small-volume droplet of solution, since the volume of the bead is far smaller than the conventional volume of the assay. Moreover, the reaction can occur more rapidly because of the smaller molecular diffusion length, since the beads are homogeneously suspended in the solution. To achieve multiplexing, it is necessary to code the beads to recognize which bead corresponds to which analyte. Various methods such as intensity of fluorescence,[12] multicolor fluorescence,[14] shape,[16] colloidal crystal,[17] metallic barcoding,[18] and surface-enhanced Raman scattering[19] have been proposed as bead-coding methods. Among these, fluorescence-based encoding is most commonly used. This may be because of the high compatibility between fluorescence-based coding and flow cytometry technology. On the other hand, image analysis-based cell counters that are capable of the quantitative measurement of fluorescence intensity, called image cytometers, are becoming more widely used in recent years. Since the image cytometer is relatively affordable and maintenance free, it is therefore an attractive choice for the detection of multiplexed bead-based assays. In this paper, we report the development of a bead-based immunoassay system, in which the size of the bead is used to code for each individual antibody, by applying an image-cytometer-based multiplexed assay.

2. Materials and Methods

2.1 Materials and apparatus

Spherical polystyrene microbeads with diameters of 10 and 20 μm (Cat #17136, 18329) were purchased from Polysciences, Inc., USA. Goat anti-mouse IgG (Prod#31164) was purchased from Invitrogen, USA. Mouse IgG (Prod#31903) was purchased from Pierce. A goat anti-mouse IgG fluorescein isothiocyanate (FITC) conjugate (Cat #02-18-06) was purchased from KPL. A goat anti-rat IgG (Prod#31220) was purchased from Invitrogen. Rat IgG (Prod#14131) was purchased from Sigma-Aldrich Co., LLC. Goat anti-rat IgG FITC conjugate (Cat#02-16-06) was purchased from KPL. The enzyme-linked immunosorbent assay (ELISA) kit for human albumin (Cat # E80-129) was purchased from Bethyl Laboratories Inc. Goat anti-human albumin IgG FITC conjugate (Cat # A80-129F) was purchased from Bethyl Laboratories Inc. Bovine serum albumin (BSA, A7030) was purchased from Sigma-Aldrich Co., LLC. Polyoxyethylene[20] sorbitan monolaurate (Tween20, Cat#167-11515) was purchased from Nacalai Tesque Inc. Dulbecco's phosphate-buffered saline (DPBS) was prepared at the standard concentration and the pH was adjusted to 7.4. Polydimethylsiloxane (PDMS, Silpot 184) was purchased from Dow Corning Toray Co., Ltd. Microcover glass (No. 1) was purchased from Matsunami Glass Ind., Ltd. The inverted microscope used for fluorescence microscopy was the Olympus Corporation IX 71 with an X20 objective lens (YLCPlanFL N, NA 0.45, Olympus). A scientific complementary metal oxide semiconductor (sCMOS) digital camera (Orca flash 4.0, C11440, Hamamatsu Photonics) was used to obtain fluorescent images. A Cellometer K2 (Nexcelom) image cytometer was used for image cytometric analysis.

2.2 Preparation of antibody-immobilized microbeads

200 μl of microbeads was added to each sample tube. The beads were pelleted by centrifugation at 1000 × *g* for 1 min, and the supernatant was removed by aspiration. The

microbead pellet was then washed three times in 200 µl of DPBS by centrifugation at 1000 × *g* for 1 min. After the final wash, the microbead pellet was resuspended in 20 µl of DPBS. A 20 µl aliquot of undiluted antibody solution was applied to a new 2 ml low-protein-binding reaction tube. The washed microbeads were resuspended by sonication for 5 min. A 2 µl aliquot of the washed microbeads in suspension was added into the antibody solution and gently mixed by vortexing, followed by sonication for 5 min. The physical adsorption process was then carried out on a rotary mixer at room temperature for more than 24 h. A 1 ml aliquot of 0.05% Tween 20 in DPBS solution (v/v) was added to the reaction tube and the tube was then centrifuged at 1000 × *g* for 1 min, before the supernatant was removed. This procedure was carried out three times to wash the microbeads. The microbeads were then blocked by adding 1 ml of 1% BSA in DPBS solution (w/v) and incubating at 4 °C overnight.

2.3 Immunoassay procedure

Antibody-immobilized microbeads were pelleted by centrifugation at 1000 × *g* for 1 min and the supernatant was removed. The microbeads were then washed twice by the addition of 1 ml of 0.05% Tween 20 in DPBS and centrifugation at 1000 × *g* for 1 min. The beads were then homogeneously resuspended by vortexing in 1 ml of 0.05% Tween 20 in DPBS. The microbeads were then dispensed into new reaction tubes by adding 100 µl of each antibody. The mixed suspension of microbeads was then pelleted by centrifugation, and resuspended at the preferred concentration in 1% BSA in DPBS, before 100 µl of sample solution was added into corresponding reaction tubes for immunoreaction. The immunoreaction was incubated for 1 h with mixing at room temperature. All tubes were centrifuged, and the supernatant was removed by aspiration. The beads were washed in triplicate by the addition of 1 ml of 0.05% Tween20 in DPBS and centrifugation at 1000 × *g* for 1 min. FITC conjugates corresponding to each analyte were diluted 1:10 in 1% BSA in DPBS, and 100 µl of the dilution was added into each reaction tube for each, followed by incubation with mixing at room temperature. All reaction tubes were then centrifuged at 1000 × *g* for 1 min and the supernatant was removed by aspiration. The microbeads were again washed in triplicate by the addition of 1 ml of 0.05% Tween 20 in DPBS and centrifugation at 1000 × *g* for 1 min. Microcover glass slides attached to 1-mm-thick PDMS sheets that were punched with 3 mm holes were prepared for fluorescent microscopy. A 5 µl aliquot of the bead suspension was added into each hole, and the fluorescent images were obtained using a fluorescent microscope with a sCMOS digital camera. Each image was acquired with an exposure time of 1 s and binning setting of 4. A one-sixth neutral density (ND) filter was used to adjust the brightness of excitation light to minimize bleaching of FITC. An exposure time of 1 s was used to acquire the image for image cytometry.

3. Results and Discussion

3.1 Multiplexed immunoassay of mouse and rat IgG

The results of the multiplexed immunoassay with mouse and rat IgG are shown in Fig. 1. The samples were a mixture of rat and mouse IgG at various concentrations, dissolved in 1% BSA in DPBS solution. The relationship between the fluorescence intensity of the microbeads and sample concentration is shown in Fig. 1(a). Anti-mouse and anti-rat IgG antibodies were immobilized

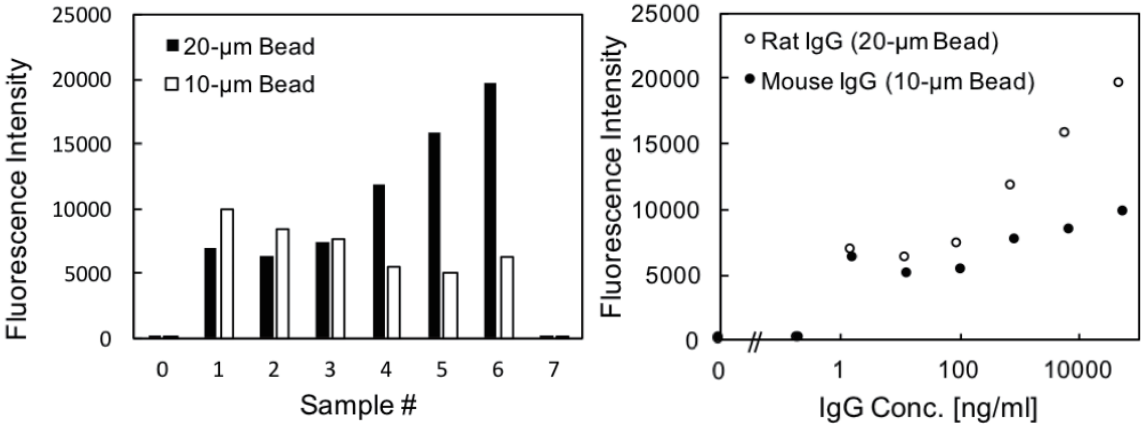

Fig. 1. (a) Fluorescent intensity of anti-mouse IgG antibody-immobilized microbeads (10 μm) and anti-rat IgG antibody-immobilized microbeads (20 μm) reacted with mixtures of rat and mouse IgG at various concentrations. (b) Calibration curves plotting the relationship of fluorescent intensity of 10 μm microbeads with the concentration of mouse IgG and fluorescent intensity of 20 μm microbeads with concentration of rat IgG.

onto 10 and 20 μm microbeads, respectively. Figure 1(b) shows the calibration curve for each IgG, obtained by plotting the relationship between the fluorescence intensity of the microbeads and the concentration of the target molecule, which is mouse IgG in the case of 10 μm microbeads and rat IgG in the case of 20 μm microbeads. We observed a clear increasing trend between the fluorescence intensity in response to the concentration of IgG. However, this trend is inverted at relatively low concentration ranges of around 1–10 ng/ml, while blank samples show the lowest signal intensity. To investigate the reason behind this, we carried out experiments on probing nonspecific signals (Fig. 2). The closed square plots show the calibration curves obtained using antibody-free microbeads, for which the immobilization process was carried out using antibody-free antibody solution. These calibration curves show the relationship between the concentrations of rat and mouse IgG in Figs. 2(a) and 2(b), respectively. The surface of the microbeads was blocked with BSA where no antibody was immobilized. As the calibration curves indicate, it is clear that fluorescence does not change in relation to the concentration of IgGs. Therefore, nonspecific signals due to the nonspecific physical adsorption of molecules onto the microbead surface can be ignored in this system. Next, the relationship between fluorescence intensity and concentration of IgG was measured. While rat IgG was measured using anti-mouse IgG antibody-immobilized microbeads, mouse IgG was measured using anti-rat IgG antibody-immobilized microbeads [Figs. 2(a) and 2(b)]. Therefore, cross-reactivity could be confirmed from the open circular plots. Calibration curves show a gradual response, increasing by around 100 ng/ml with increasing concentration of IgG in both cases. Our conclusion that the adsorption on the surface of the microbeads is specific suggests that this response arises owing to cross-reactivity between antigens and antibodies. Therefore, we concluded that the signal shown at around 1-10 ng/ml in Fig. 1 is due to cross-reactivity, which highlights the importance of the choice of antibody and matching of antigens in multiplexed immunoassay systems.

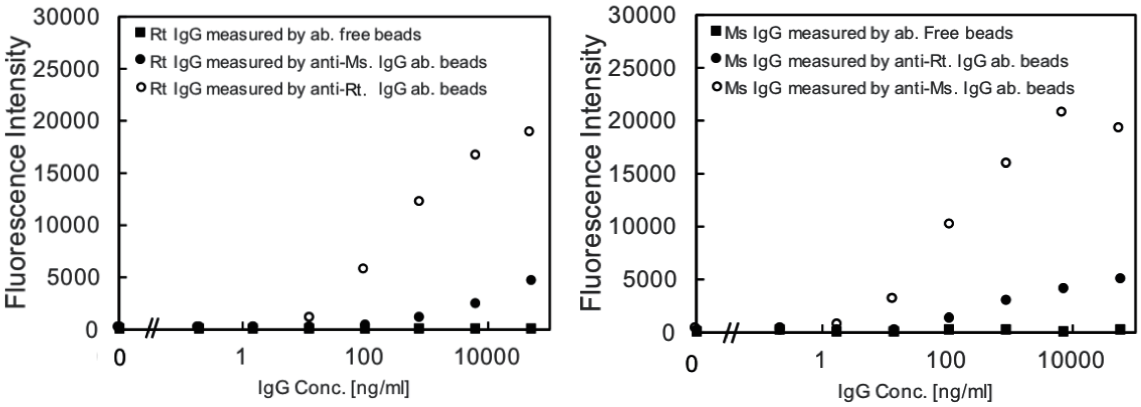

(a) (b)

Fig. 2. Selectivity of antibody and antigen used in this study. (a) Reactivity of rat IgG to microbeads with various antibody immobilization conditions. The closed square plot indicates the case of antibody-free beads. The closed circular plot indicates the case of anti-Ms IgG antibody-immobilized beads. The open circular plot indicates the case of anti-Rt IgG antibody-immobilized beads. (b) Reactivity of mouse IgG to microbeads under various antibody immobilization conditions. The closed square plot indicates the case of antibody-free beads. The closed circular plot indicates the case of anti-Rt IgG antibody-immobilized beads. The open circular plot indicates the case of anti-Ms IgG antibody-immobilized beads.

3.2 Multiplexed immunoassay of mouse IgG and human albumin and demonstration of image cytometry

The issue of the cross-reactivity between immunoreaction systems of mouse and rat IgG was emphasized in the previous section. We therefore tested a more selective immunoreaction by using mouse IgG and human albumin, and demonstrated image-cytometry-based multiplexed analysis (Fig. 3). Anti-mouse IgG and anti-human albumin were immobilized onto 10 and 20 μm microbeads, respectively. Samples were a mixture of mouse IgG and human albumin at various concentrations and dissolved in 1% BSA DPBS solution. Figure 3(a) shows a fluorescent image of these microbeads. The fluorescence intensity of each microbead suspended in each sample is shown in Fig. 3(b). Calibration curves, showing the relationship between the fluorescence intensity of 10 μm microbeads and the concentration of mouse IgG, and the relationship between the fluorescence intensity of 20 μm microbeads and the concentration of human albumin, are shown in Fig. 3(c). As the calibration curves indicate, there is a clear relationship between fluorescence intensity and the concentration of the analyte. We observed an inverse response in the low concentration range of around 1–10 ng/ml in the case of human albumin; however, the calibration curve of the mouse IgG shows an increasing response over the entire range of measurement, suggesting no cross-reactivity with human albumin. The result of the image cytometric analysis of this immunoassay is shown in Fig. 4. The horizontal axis of the figures shows the measured size of the microbeads and the vertical axis shows the fluorescence intensity of the microbeads. In the case of image cytometric analysis of both mouse IgG and human albumin, we observed an increased response to the concentration of the analyte, which suggests that there is no cross-reactivity in any immunoreaction system in this case. Thus, we have successfully demonstrated a simple, size-coded multiplexed bead-based immunoassay using image cytometric analysis.

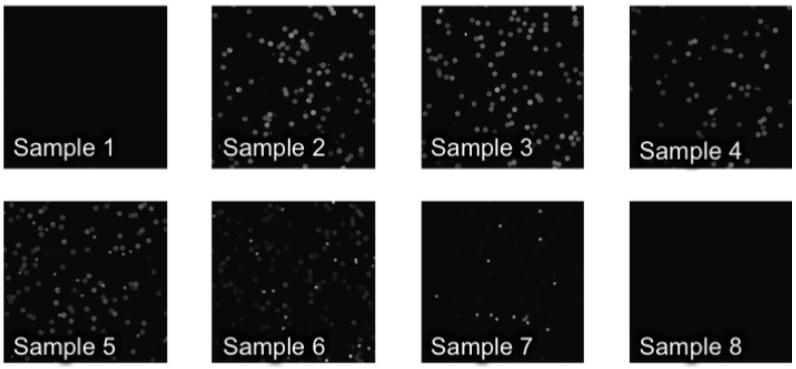

(a)

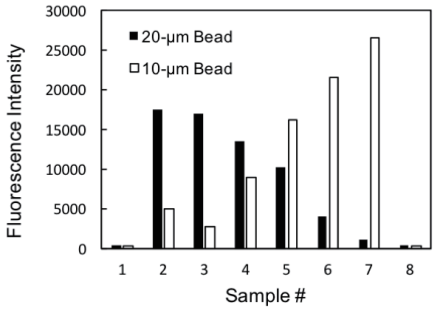

(b)

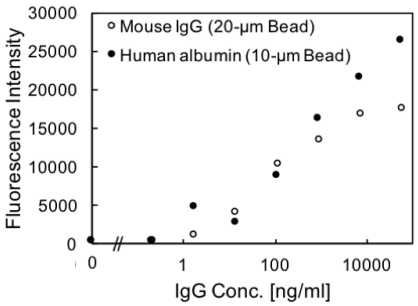

(c)

Fig. 3. (a) Fluorescence image of microbeads after immunoreactions. (b) Immunoreaction of the anti-human albumin antibody-immobilized microbeads (10 μm) and the anti-mouse IgG antibody-immobilized microbeads (20 μm) with a mixture of mouse IgG and human albumin at various concentrations. (c) Calibration curves plotting the relationship between fluorescence of the 10 μm microbeads and the concentration of human albumin, and fluorescence of 20 μm microbeads and the concentration of mouse IgG.

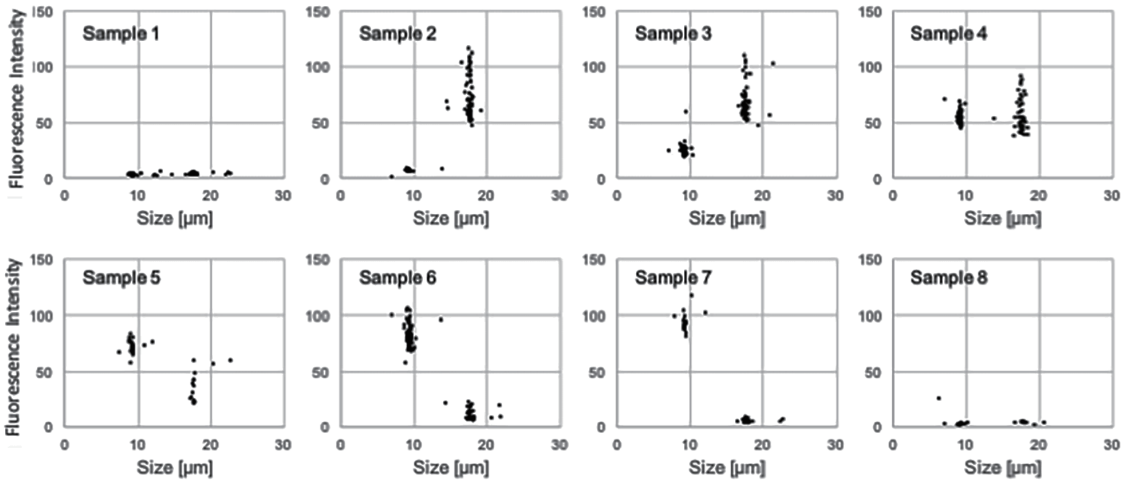

Sample #	1	2	3	4	5	6	7	8
Mouse IgG conc. (ng/ml)	0	58000	7250	906	113	14	1.8	0.2
Human albumin conc. (ng/ml)	0.21	1.68	13.4	107	860	6875	55000	0

Fig. 4. Result of image cytometric analysis of multiplexed immunoreaction of mouse IgG and human albumin.

4. Summary

In this study, we demonstrated a duplexed bead-based immunoassay using image cytometric analysis. We developed the multiplexed immunoassay system presented here for the measurement of rat and mouse IgG, although we observed cross-reactivity in this immunoreaction system. We then developed another multiplexed immunoassay system with mouse IgG and human albumin, which demonstrated even less cross-reactivity, and applied the immunoassay system to image cytometric analysis to establish a simple, size-coded multiplexed bead-based immunoassay system. Image cytometry is maintenance free and has lower running costs compared with flow cytometry. We thus conclude that we have demonstrated a promising system that is low cost and maintenance free, enabling multiplexed bead-based immunoassay based on image cytometric analysis.

References

1 T. T. Ngo and H. M. Lenhoff: Mol. Cell. Biochem. **44** (1982) 3.
2 K. Sato, M. Tokeshi, H. Kimura, and T. Kitamori: Anal. Chem. **73** (2001) 1213.
3 B. S. Lee, J.-N. Lee, J.-M. Park, J.-G. Lee, S. Kim, Y.-K. Cho, and C. Ko: Lab Chip **9** (2009) 1548.
4 A. Apilux, Y. Ukita, M. Chikae, O. Chailapakul, and Y. Takamura: Lab Chip **13** (2013) 126.
5 S. F. Kingsmore: Nat. Rev. Drug Discov. **5** (2006) 310.
6 M. Sugimoto, D. T. Wong, A. Hirayama, T. Soga, and M. Tomita: Metabolomics **6** (2010) 78.
7 Z. J. Sahab, S. M. Semaan, and Q.-X. A. Sang: Biomarker Insights **2** (2007) 21.
8 B. B. Haab: Current Opinion Biotechnol. **17** (2006) 415.
9 A. Carlssona, C. Wingrena, J. Ingvarssona, P. Ellmarka, B. Baldertorpc, M. Fernöc, H. Olssonc, and C. A. K. Borrebaecka: Eur. J. Cancer **44** (2008) 472.
10 S. Pang, J. Smith, D. Onley, J. Reeve, M. Walker, and C. Foy: J. Immunol. Methods **302** (2005) 1.
11 M. R. Henry, P. Wilkins Stevens, J. Sun, and D. M. Kelso: Anal. Biochem. **276** (1999) 204.
12 E. Morgan, R. Varro, H. Sepulveda, J. A. Ember, J. Apgar, J. Wilson, L. Lowe, R. Chen, L. Shivraj, A. Agadir, R. Campos, D. Ernst, and A. Gaur: Clin. Immunol. **110** (2004) 252.
13 Y. Zhao, Y. Cheng, L. Shang, J. Wang, Z. Xie, and Z. Gu: Small **11** (2015) 151.
14 N. Theilacker, E. E. Roller, K. D. Barbee, M. Franzreb, and X. Huang: J. R. Soc. Interface **8** (2011) 1104.
15 S. Birtwell and H. Morgan: Integrative Biol. **1** (2009) 345.
16 D. C. Pregibon, M. Toner, and P. S. Doyle: Science **315** (2007) 1393.
17 X. Zhao, Y. Cao, F. Ito, H.-H. Chen, K. Nagai, Y.-H. Zhao, and Z.-Z. Gu: Angew. Chem. Int. Ed. **45** (2006) 6835.
18 S. R. Nicewarner-Peña, R. G. Freeman, B. D. Reiss, L. He, D. J. Peña, I. D. Walton, R. Cromer, C. D. Keating, and M. J. Natan: Science **294** (2001) 137.
19 G. Bodelón, V. Montes-García, C. Fernández-López, I. Pastoriza-Santos, J. Pérez-Juste, and L. M. Liz-Marzán: Small **11** (2015) 4149.